JOURNAL OF AIRCRAFT
Vol. 31, No. 3, May–June 1994

Navier-Stokes Computations for Oscillating Control Surfaces

Shigeru Obayashi* and Guru P. Guruswamy†
NASA Ames Research Center, Moffett Field, California 94035

Unsteady Navier-Stokes computations have been performed for simulating transonic flows over wings with oscillating control surfaces using a locally moving grid and a stationary-mismatched zoning scheme. An F-5 wing and a clipped delta wing are chosen for the present study. The computed unsteady pressures and the response characteristics to the control surface motions are compared with experimental data. The results successfully predict main features of the unsteady pressure profiles, such as the double peaks at the shock wave and at the hinge line.

Introduction

AIRCRAFT are often subject to aerodynamic oscillation, especially in the transonic regime, because of flow nonlinearities and the presence of the moving shock waves. In this unsteady aerodynamics environment, aircraft rely heavily on active controls for safe and steady flight operation. Active control is also needed for the suppression of structural flutter and the reduction of structural weight to achieve stable flight conditions.

The influence of control surfaces on both aerodynamics and aeroelastic performance of a wing is more pronounced in the transonic regime. These influences can be constructively used to improve the wing performance through proper maneuvering of the active control surfaces. Active control technology relies on accurate predictions of unsteady aerodynamics and aeroelastic performance of a wing. Since the experimental evaluation of the effect of a control surface on the wing performance would involve considerable cost and the risk of structural damage in a wind tunnel, it is necessary to initiate the investigation through theoretical analyses.

The theoretical analysis of transonic flows is complicated by the presence of mixed subsonic and supersonic regions within the flowfield. For an unsteady flowfield, such as that surrounding a control surface, additional considerations are needed to treat moving shock waves of varying strength and subsequent flow separation induced by the shock-wave/boundary-layer interactions. For the case of the control surface in which viscous effects dominate, computation based on the unsteady Navier-Stokes equations is needed.

The physics of unsteady transonic flow around a control surface has been simulated at various levels of inviscid and viscous approximations using small disturbance theory[1,2] and, for limited two-dimensional cases, the unsteady Navier-Stokes equations.[3,4] The purpose of this study is to explore the capability of three-dimensional Navier-Stokes simulation for the unsteady flowfield surrounding a wing with an oscillating control surface.

The present investigation is initiated in conjunction with a recently developed code, ENSAERO, which is capable of computing aeroelastic responses by simultaneously integrating the Euler/Navier-Stokes equations and the modal structural equations of motion using aeroelastically adaptive dynamic grids.[5–8] The code has been applied to transonic flows from small to moderately large angles of attack for fighter wings undergoing unsteady motions. In this article, the geometric capability of the code is extended to simulate unsteady flows over a rigid wing with an oscillating trailing-edge flap.

To model an oscillating control surface efficiently, an algebraic grid generation technique is incorporated into the code. The grid moves every time step to follow the deflection of the control surface. Small deflections are handled using a sheared single grid, and large deflections are handled using a zonal technique.[9]

In this article, the first test case considers transonic flows over an F-5 wing with an oscillating inboard control surface. The same case was simulated using the small disturbance theory in Ref. 2. The second case considers transonic vortical flows over a clipped delta wing. Unsteady Navier-Stokes computations for the clean wing were reported in Ref. 8. The mismatched zonal cases are demonstrated for this case.

Numerical Method

Governing Equations and Discretization

The nondimensionalized Reynolds-averaged, thin-layer Navier-Stokes equations used in this study can be written in conservation-law form in a generalized body-conforming curvilinear coordinate system for three dimensions as follows:

$$\partial_\tau \hat{Q} + \partial_\xi \hat{E} + \partial_\eta \hat{F} + \partial_\zeta \hat{G} = (1/Re)\partial_\zeta \hat{G}^v \qquad (1)$$

where $\tau = t$, $\xi = \xi(x, y, z, t)$, $\eta = \eta(x, y, z, t)$, and $\zeta = \zeta(x, y, z, t)$. In this article, the ξ and η directions are along the streamwise and spanwise directions, respectively, of a wing. The viscous derivatives associated with these directions are dropped. The ζ direction is normal to the wing surface, and thus the viscous derivatives are retained.

In Eq. (1), $\hat{Q}$ is the vector of conserved quantities, $\hat{E}$, $\hat{F}$, and $\hat{G}$ are the inviscid flux vectors, and $\hat{G}^v$ is the thin-layer viscous flux vector. The viscosity coefficient in $\hat{G}^v$ is computed as the sum of the laminar and turbulent viscosity coefficients where the laminar viscosity is taken from the freestream laminar viscosity, assumed to be constant for transonic flows. As an option, Sutherland's law can be used to calculate the laminar viscosity. The turbulent viscosity is evaluated by the Baldwin-Lomax algebraic eddy-viscosity model.[10] Since the flowfield to be considered in this article contains leading-edge separation, it is important to apply a modification to the turbulence model originally developed for cross-flow-type separation.[11]

In this study, a conventional finite difference (FD) grid system is used. However, for the moving grid case, it is im-

Received Aug. 4, 1992; presented as Paper 92-4431 at the AIAA Atmospheric Flight Mechanics Conference, Hilton Head, SC, Aug. 10–12, 1992; revision received May 27, 1993; accepted for publication May 27, 1993.

*Senior Research Scientist, MCAT Institute, San Jose, CA. Senior Member AIAA.
†Research Scientist. Associate Fellow AIAA.

portant to treat the time metrics correctly. The FD formulation does not give freestream-capturing time metrics.[12,13] The FD time metrics are related to the grid velocity, e.g.

$$\xi_t = -\xi_x x_t - \xi_y y_t - \xi_z z_t \tag{2}$$

For rigid motion of the grid, the freestream can be preserved by applying a freestream subtraction technique to the time metric terms.

In the finite volume (FV) formulation, the right side of Eq. (2) is expressed as a product of a surface vector and a grid velocity. The time integration of the product from time level n to $n + 1$ represents a volume swept by the surface during one time step. By computing this volume, $V_{\xi n}^{n+1}$, the freestream-capturing time metrics can be obtained as

$$\frac{\xi_t}{J} = -\frac{V_{\xi n}^{n+1}}{\Delta t} \tag{3}$$

(see Ref. 13 for more details). Because control surfaces oscillating at a small amplitude were considered in this article, the FD and FV formulas did not produce any significant difference in the results.

Upwind Algorithm

Several numerical schemes have been developed to solve Eq. (1). The present code has two different schemes: 1) the central-difference and 2) the streamwise upwind schemes. In this work, a streamwise upwind algorithm is applied to compute the inviscid cell-interface fluxes. The streamwise upwind algorithm has recently been developed and applied to steady and unsteady problems of transonic flows over wings, including flexibility of the wing.[7,8] A third-order evaluation is used for the inviscid term. A second-order, central-difference evaluation is applied to the viscous term. The complete algorithm can be found in Ref. 7.

An implicit method is used for the time integration because it is more suitable for expensive unsteady viscous calculations. The method chosen for the upwind scheme is the lower-upper factored, alternating direction implicit (LU-ADI) method.[14] The method is first-order accurate in time and requires only scalar bidiagonal matrix inversions (see Refs. 14 and 15 for additional details).

Specific code performance information for the current study is given as follows. All results were computed on either a Cray Y-MP or Cray-2 computer at NASA Ames Research Center. The performance of the upwind version of ENSAERO is 170 MFLOPS and 19 μs per iteration per grid point on a single Cray Y-MP processor.

Control Surface Grid

In this article, a single C-H topology grid for a wing with a control surface is used. In each C grid section, a two-dimensional algebraic grid generation technique is applied to each airfoil section.[16] At both ends of the control surface, a small gap is introduced (Fig. 1). Flow-through condition is applied to the grid points within the gap region. In this region, the grid is sheared to model the control surface movement. The region is represented by using three spanwise grid points in the following calculations. The size of the gap can be minimized by clustering the grid in this region, and therefore its effect on the overall solution can be reduced.

The C grid around a deflected control surface can be obtained in two ways. One is to shear every grid line normal to the control surface with the local deflection, Δx and Δz. The other is to regenerate the entire C grid with the control surface deflected at every time step. The computational overhead of the latter approach is only 7% because of the efficient algebraic grid generation scheme. However, the computed surface pressures did not show any differences between the two methods. Thus, the results presented in this article were computed using the shearing technique.

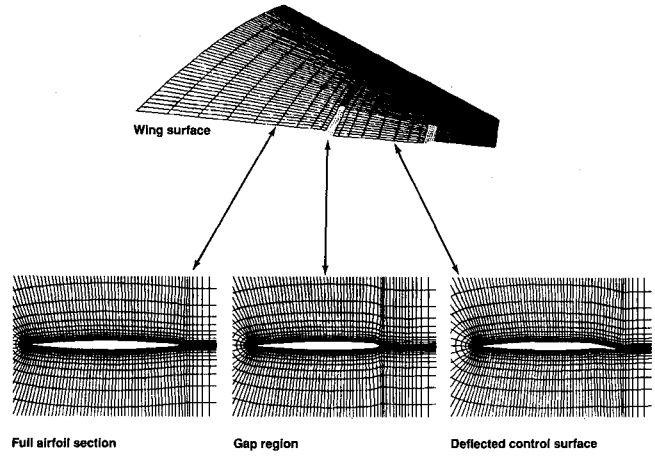

Fig. 1 Single grid for a wing with a control surface.

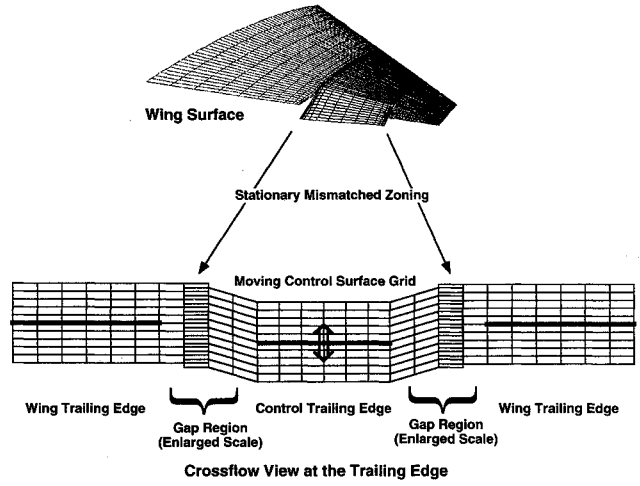

Fig. 2 Zonal grids for a wing with a control surface.

Zonal Grid Capability

The present code inherits the zonal grid capability developed for the transonic Navier-Stokes (TNS) code to handle complicated geometries, such as complete aircraft configurations.[9] Although a problem with the extension of the zonal method to unsteady flows was reported in a previous paper,[17] a code error was found and has been corrected. In the present study, the corrected code is used.

In this article, a mismatched zoning scheme is introduced to accommodate large mean flap deflections, while a shearing-grid technique is used to model an oscillating flap about the mean deflection. Zonal interfaces are located at both ends of a control surface including the gap (Fig. 2). As the control surface deflects, the grids become mismatched. However, if the zonal interfaces move, it requires expensive computation to find interpolation coefficients on the mismatched zones at every time step. To maintain the efficiency of the single-grid computation, the zonal interfaces should remain stationary when the control surface oscillates with a small amplitude. Instead, the control surface grid shears at the gap region similar to the single-grid case. To transfer the flow information from one grid to another, bilinear interpolation is used here (see the nonconservative interpolation in Ref. 18), because the present zonal interfaces are coplanar. Although the present interpolation is explicit and nonconservative, the error can be ignored since practical time-step sizes used for Navier-Stokes computations are small.

A different zonal approach is reported in Ref. 19 to treat a stationary, deflected flap. Its extension to oscillating control surfaces will be investigated in the near future.

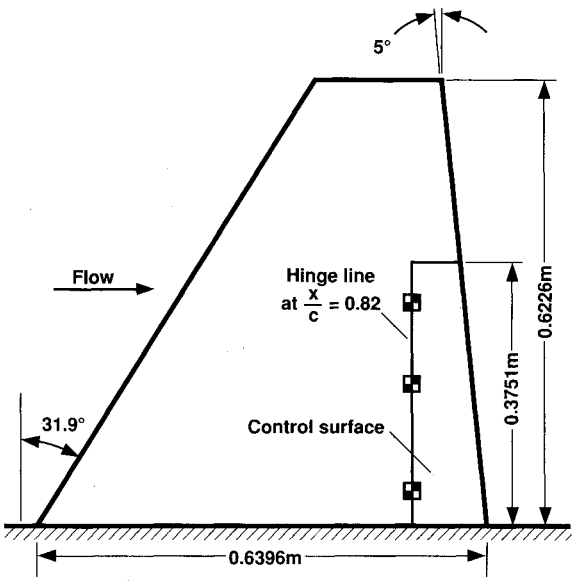

Fig. 3 Planform of F-5 wing with inboard trailing-edge flap.

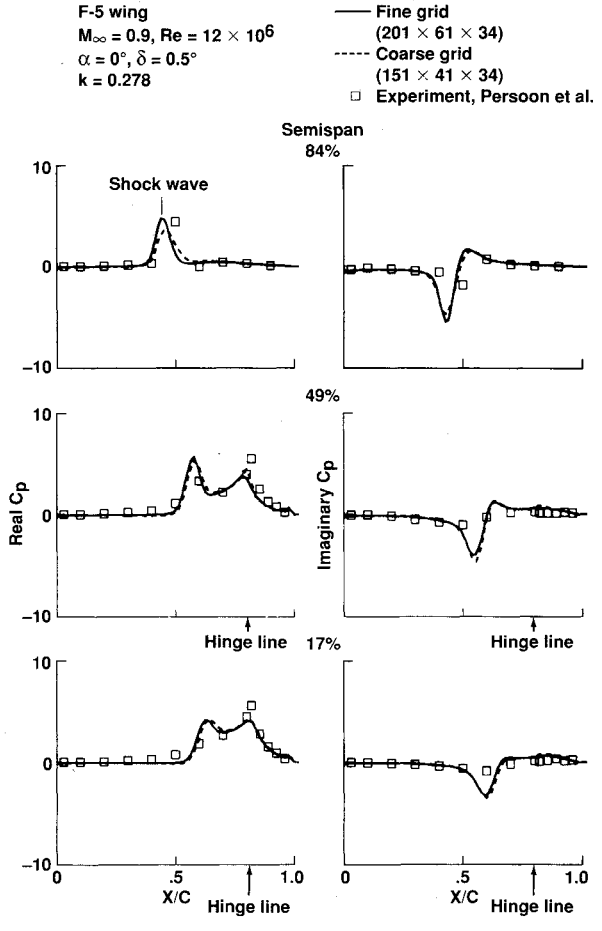

Fig. 4 Comparison of computed unsteady pressures between the coarse- and fine-grid solutions on the upper surface of the F-5 wing.

Results

F-5 Wing

The first test considers unsteady viscous flows over an F-5 wing with an oscillating inboard control surface. This wing has an aspect ratio of 2.98, a taper ratio of 0.31, and a leading-edge sweep angle of 31.92 deg. Computations were made using coarse and fine grids containing 151 × 41 × 34 points and 201 × 61 × 34 points, respectively. The wing planform is given in Fig. 3. It should be noted that the present C-H

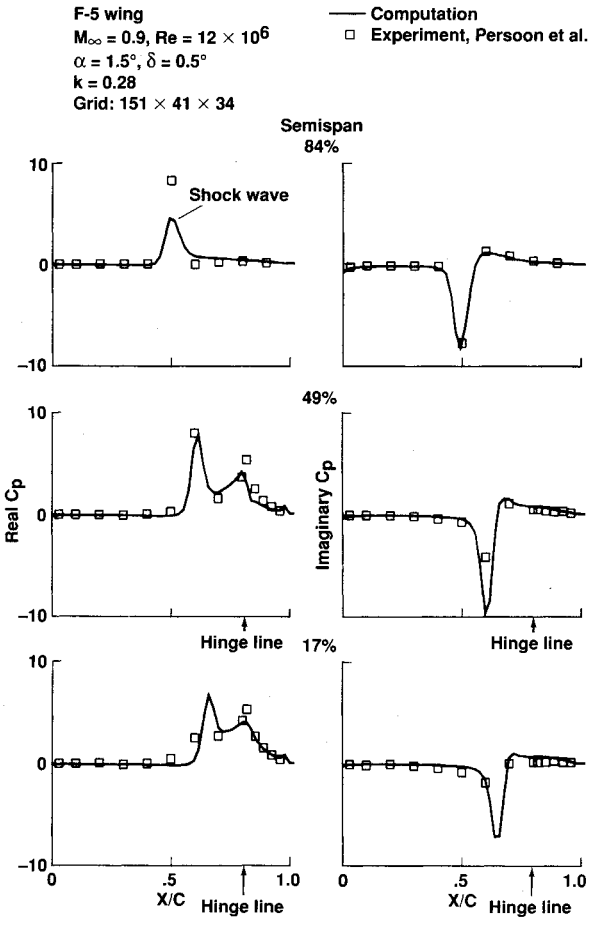

Fig. 5 Comparison of computed unsteady pressures with experimental data on the upper surface of the F-5 wing.

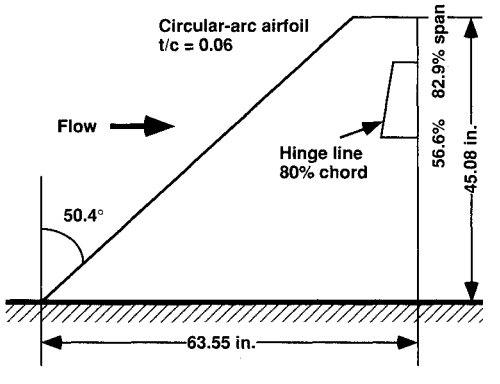

Fig. 6 Planform of clipped delta wing with trailing-edge flap.

grid does not have enough resolution for the faired wingtip of the experimental model. The control surface is oscillating about an axis located at the 82% root chord, and the hinge axis is normal to the wing root. The test cases are at a Mach number of $M_\infty = 0.9$, where the experimental steady and unsteady data are given in Ref. 20. All F-5 wing cases are computed at a Reynolds number based on the root chord of $Re_\infty = 12 \times 10^6$.

The response of surface pressure to the control surface motion can be represented in terms of real and imaginary parts of the first Fourier component of the unsteady pressures. In Fig. 4, the coarse- and fine-grid results are compared with experimental data at an angle of attack of $\alpha = 0$ deg, with the control surface oscillating at a frequency of 20 Hz and an amplitude of $\beta = 0.5$ deg. This frequency corresponds to a reduced frequency of $k \cong 0.28$. Results are shown for the upper surface pressures at three spanwise locations. It is noted

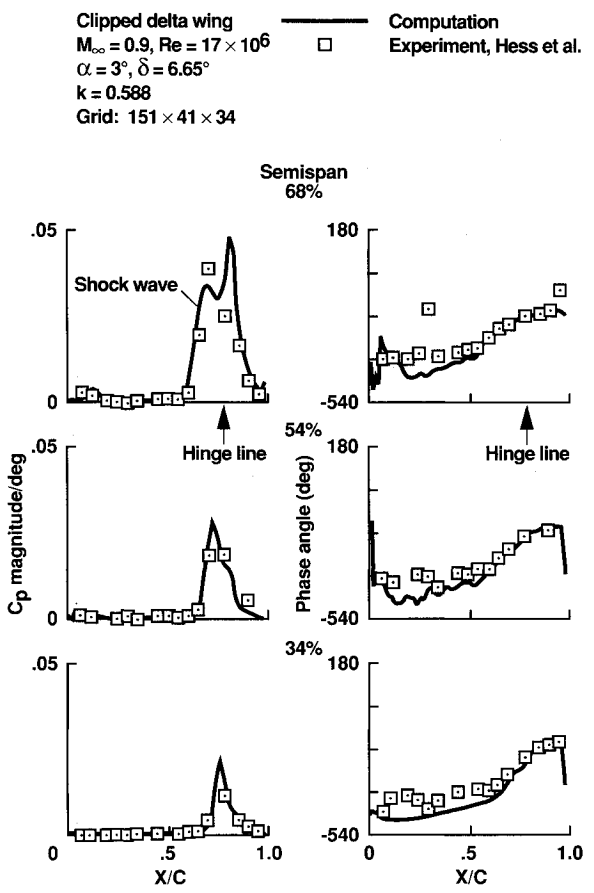

Fig. 7 Comparison of computed unsteady pressures with experimental data on the upper surface of the clipped delta wing.

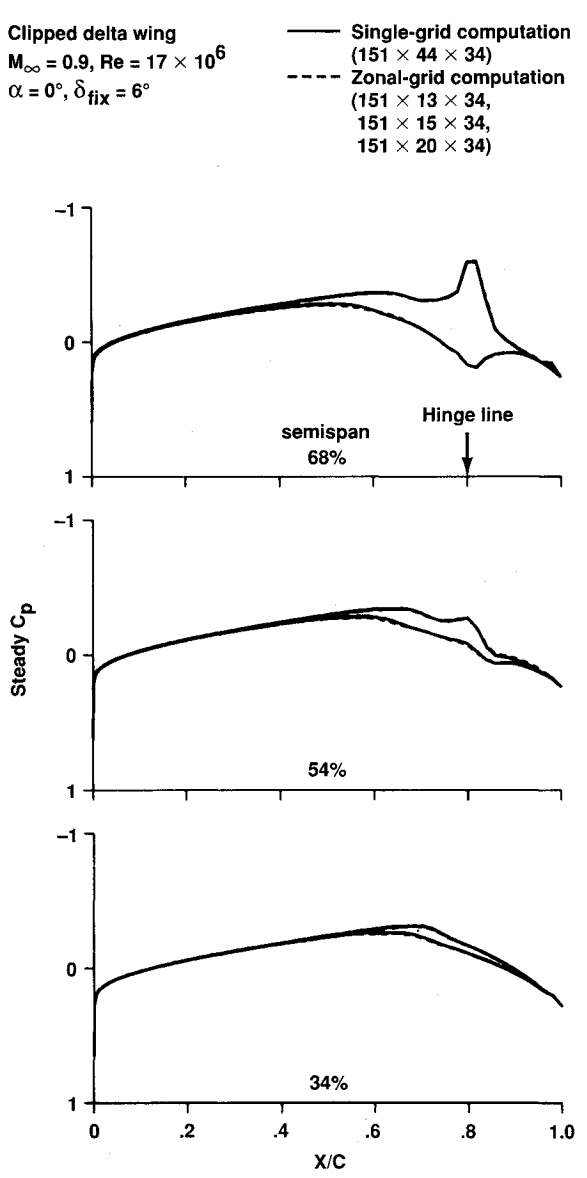

Fig. 8 Comparison of computed steady pressures between the single and zonal grids over the clipped delta wing.

that for $M_\infty = 0.9$, the steady-state solution is shock-free except near the wingtip. The spikes in the unsteady pressure distributions around the 50% chord indicate the motion of the shock wave due to the control surface oscillation. The spikes are also seen at the hinge line. In the real part of the unsteady pressures, at the inboard sections, the computations predict higher spikes for the motion of the shock wave than observed in the experiment. This is because the computation assumes a plane of symmetry at the root section, while the experiment has a solid wall. In contrast, the computations predict lower spikes at the hinge line. This is because the present grid has constant chordwise distributions and therefore does not align to the hinge line. In the imaginary part, there is a greater discrepancy between the computation and the experiment, which is possibly due to the resolution of the experimental data as shown later. The coarse- and fine-grid results show reasonably good agreement in Fig. 4.

The unsteady pressure profiles using time-step sizes yielding 1800 and 2400 steps/cycle were compared with each other to check the time-step dependency of the coarse-grid results. The unsteady results converged at 1800 steps/cycle, and thus this time step was used for the F-5 wing results shown in this article. The finite difference time metrics, Eq. (2), and the freestream-capturing time metrics, Eq. (3), were checked on the coarse grid as well. No difference was found for this small amplitude of control surface oscillation.

Figure 5 shows the unsteady results on the coarse grid at 1.5-deg angle of attack with the flap oscillating at a frequency of 20 Hz and an amplitude of 0.5 deg at three spanwise locations. The real part of the unsteady pressures follows the previous observation for Fig. 4. The imaginary part shows better agreement at the outboard section than Fig. 4. Since the computed results show more consistent trends, the disagreement in the imaginary part is likely due to the resolution of the experimental data.

Clipped Delta Wing

The next test case considers a clipped delta wing with an oscillating trailing-edge control surface.[21] The wing planform is shown in Fig. 6. The wing has a leading-edge sweep angle of 50.4 deg and a 6%-thick circular-arc airfoil section. At $M_\infty = 0.9$ and $\alpha = 3$ deg, both a leading-edge vortex and a shock wave are present on the upper surface of the wing. The present C-H grid contains 151 × 44 × 34 points (see Fig. 1). Since the experiment was conducted using a Freon test medium, the ratio of specific heats γ is set to 1.135 in the following computations. In addition, the modified Baldwin-Lomax model is used to account for the leading-edge vortex. Steady-state and rigid pitching calculations of this wing were reported in Ref. 8. Although three cases were computed for this oscillating control surface with an amplitude of 2.20, 4.38, and 6.65 deg, the 6.65-deg case is discussed in the following because the other two cases show similar trends.

Figure 7 shows the unsteady pressures with the control surface oscillating at a frequency of 8 Hz and an amplitude of 6.65 deg at $M_\infty = 0.9$, $\alpha = 3$ deg, and $Re_c = 17 \times 10^6$, based on the root chord. Results are shown as magnitude and phase angle of the upper surface pressure responses at three spanwise sections. The magnitude part of the unsteady pressures shows significant influence of the control surface oscillation. At the 68% spanwise section, the plot shows double

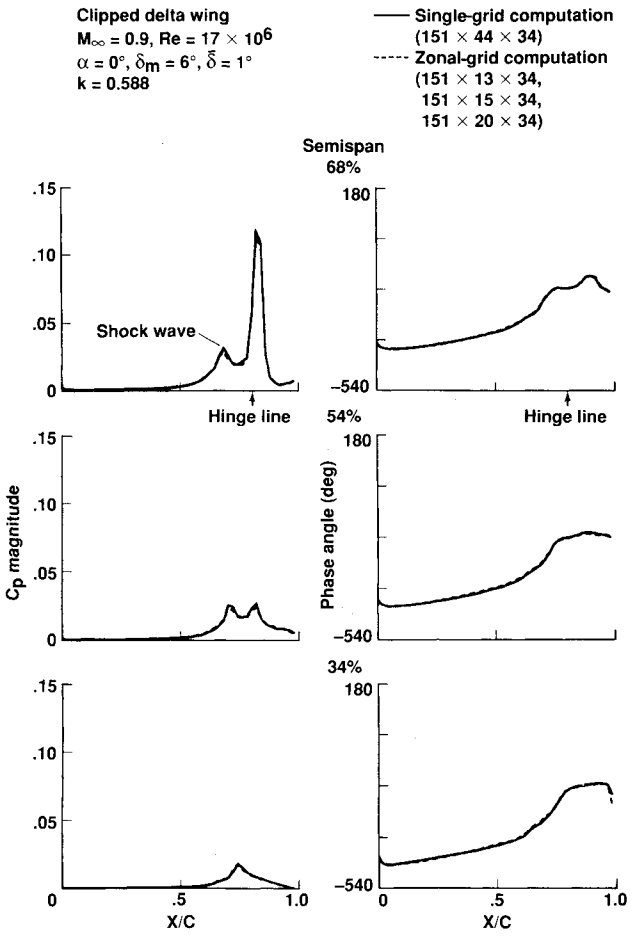

Fig. 9 Comparison of computed unsteady pressures between the single and zonal grids on the upper surface of the clipped delta wing.

peaks, similar to the F-5 wing case. These correspond to the shock wave location and the control-surface hinge line. Although the computed result shows a much smaller peak due to the shock wave at the 68% section, it is consistent with the steady-state result where the shock wave appears weaker.[8] This discrepancy originates in both the experimental and computational modeling. For example, there was a misalignment of the control surface on the order of 2 deg in the experiment.[21] In contrast, the computed peak at the hinge line is much higher than the experiment. This is because the grid aligns to the hinge line in this case and the experimental data does not have enough resolution near the hinge line. The phase angle plots show a discrepancy near the leading edge. It should be noted that the computation assumes a fully turbulent flow while the experiment has a fixed transition at the 8% chord. Overall, the computed results show reasonably good agreement with the experiment.

The test case presented in Fig. 7 was more sensitive to time-step sizes. Most of the unsteady pressures on the wing surface converged at 3600 steps/cycle (the same number as the rigid pitching case in Ref. 8). However, the oscillation of the control surface caused a minor fluctuation to the leading-edge vortex, and thus, the unsteady pressures under the leading-edge vortex required 5000 steps/cycle to converge.

Zonal Grid

The zonal test case is taken from the previous clipped delta wing. The control surface is deflected 6 deg and undergoes an oscillatory motion with an amplitude of 1 deg and a frequency of 8 Hz at $M_\infty = 0.9$, $\alpha = 0$ deg, and $Re_c = 17 \times 10^6$. Because no experimental data is available for this particular case, zonal-grid results are compared with single-grid results.

First, the single grid of 151 × 44 × 34 points is divided into three zones at the gaps at both ends of the control surface. Each zone contains 151 × 13 × 34, 151 × 15 × 34, and 151 × 20 × 34 points from inboard to outboard (see Fig. 2). Special attention is given to the generation of smooth zonal interfaces because the gap region often causes skewed grid distributions.

Figure 8 shows the comparison of steady-state results between the single- and zonal-grid solutions. The control surface is deflected down 6 deg and held stationary. Asymmetric pressure distributions indicate the effects of the deflected control surface. These effects can even be seen at the inboard sections. A comparison of unsteady pressures between the single- and zonal-grid results is also given in Fig. 9. The control surface oscillates with an amplitude of $\bar{\beta} = 1$ deg about a mean deflection of $\beta_m = 6$ deg. The unsteady pressure profiles show double peaks at the shock wave and the hinge line, although the shock wave is not seen in Fig. 8. In both figures, single- and zonal-grid computations agree well, in spite of the mismatched zoning. It takes about 9 s on a Cray Y-MP single processor to set up the interpolation coefficients for all of the zonal interfaces. This corresponds to approximately two time steps of the Navier-Stokes calculation. After the coefficients are computed, the unsteady computations simply use the stored coefficients because the zonal interfaces remain stationary. This is one way to take an advantage of the flexibility of the zonal-grid technique along with the efficiency of the single-grid computation.

Conclusions

Unsteady Navier-Stokes computations have been performed for transonic flows over wings with oscillating control surfaces. To use the existing framework of the finite difference method, the time metric terms are calculated by using the finite volume concept. The use of locally moving grids has made it possible to efficiently simulate an oscillating control surface. The introduction of the stationary-mismatched zoning scheme has enhanced the capability of the code to model large deflections of control surfaces.

Comparisons of unsteady pressures with experimental data show reasonably good agreement. The computed results successfully predict main features of the unsteady pressure profiles, such as the double peaks at the shock wave and at the hinge line. In the future, an unsteady mismatched zoning scheme will be investigated. A control law will also be implemented into the code to compute aeroelastic performance of a wing.

Acknowledgments

S. Obayashi's work was supported by NASA Grant NCC 2-605. The authors would like to thank G. H. Klopfer of MCAT Institute for his helpful suggestions and discussions on the mismatched zoning scheme.

References

[1]Ballhaus, W., Goorjian, P. M., and Yoshihara, H., "Unsteady Force and Moment Alleviation in Transonic Flow," Ref. 14, Unsteady Aerodynamics, AGARD CP 227, Feb. 1978.

[2]Guruswamy, G. P., and Tu, E. L., "Transonic Aeroelasticity of Fighter Wings with Active Control Surface," *Journal of Aircraft*, Vol. 26, No. 7, 1989, pp. 682–684.

[3]Steger, J. L., and Bailey, H. E., "Calculation of Transonic Aileron Buzz," *AIAA Journal*, Vol. 18, No. 3, 1980, pp. 249–255.

[4]Horiuti, K., Chyu, W. J., and Buell, D. A., "Unsteady, Transonic Flow Computations for an Airfoil with an Oscillating Flap," AIAA Paper 84-1562, June 1984.

[5]Guruswamy, G. P., "Unsteady Aerodynamic and Aeroelastic Calculations of Wings Using Euler Equations," *AIAA Journal*, Vol. 28, No. 3, 1990, pp. 461–469.

[6]Guruswamy, G. P., "Navier-Stokes Computations on Swept-Tapered Wings, Including Flexibility," AIAA Paper 90-1152, April 1990.

[7]Obayashi, S., Guruswamy, G. P., and Goorjian, P. M., "Stream-

wise Upwind Algorithm for Computing Unsteady Transonic Flows Past Oscillating Wings," *AIAA Journal*, Vol. 29, No. 10, 1991, pp. 1668–1677; see Errata: *AIAA Journal*, Vol. 30, No. 2, 1992, p. 569.

[8]Obayashi, S., and Guruswamy, G. P., "Unsteady Shock-Vortex Interaction on a Flexible Delta Wing," AIAA Paper 91-1109, April 1991.

[9]Flores, J., and Chaderjian, N., "Zonal Navier-Stokes Methodology for Flow Simulation About a Complete Aircraft," *Journal of Aircraft*, Vol. 27, No. 7, 1990, pp. 583–590.

[10]Baldwin, B. S., and Lomax, H., "Thin-Layer Approximation and Algebraic Model for Separated Turbulent Flows," AIAA Paper 78-257, Jan. 1978.

[11]Degani, D., and Schiff, L. B., "Computations of Turbulent Supersonic Flows Around Pointed Bodies Having Crossflow Separation," *Journal of Computational Physics*, Vol. 66, No. 1, 1986, pp. 173–196.

[12]Vinokur, M., "An Analysis of Finite-Difference and Finite-Volume Formulations of Conservation Laws," *Journal of Computational Physics*, Vol. 81, No. 1, 1989, pp. 1–52.

[13]Obayashi, S., "Freestream Capturing for Moving Coordinates in Three Dimensions," *AIAA Journal*, Vol. 30, No. 4, 1992, pp. 1125–1128.

[14]Obayashi, S., "Numerical Simulation of Underexpanded Plumes Using Upwind Algorithms," AIAA Paper 88-4360, Aug. 1988.

[15]Obayashi, S., Goorjian, P. M., and Guruswamy, G. P., "Extension of a Streamwise Upwind Algorithm to a Moving Grid System," NASA TM-102800, April 1990.

[16]Obayashi, S., Matsushima, K., Fujii, K., and Kuwahara, K., "Improvements in Efficiency and Reliability for Navier-Stokes Computations Using the LU-ADI Factorization Algorithm," AIAA Paper 86-0338, Jan. 1986.

[17]Obayashi, S., Guruswamy, G. P., and Tu, E. L., "Unsteady Navier-Stokes Computations on a Wing-Body Configuration in Ramp Motions," AIAA Paper 91-2865, Aug. 1991.

[18]Klopfer, G. H., and Molvik, G. A., "Conservative Multizone Interface Algorithm for the 3-D Navier-Stokes Equations," AIAA Paper 91-1601, June 1991.

[19]Chaussee, D., and Klopfer, G., "The Numerical Study of Three-Dimensional Flow Past Control Surfaces," AIAA Paper 92-4650, Aug. 1992.

[20]Persoon, A. J., Roos, R., and Schippers, P., "Transonic and Low Supersonic Wind Tunnel Tests on a Wing with Inboard Control Surface," Air Force Flight Dynamics Lab., TR-80-3146, Dayton, OH, Dec. 1980.

[21]Hess, R. W., Cazier, F. W., Jr., and Wynne, E. C., "Steady and Unsteady Transonic Pressure Measurements on a Clipped Delta Wing for Pitching and Control-Surface Oscillations," NASA TP-2594, Oct. 1986.